Supporting Information

Facile Synthesis of Ni/NiO Composite with Superior Bifunctional Electrocatalytic Activity for Water Electrolysis Under Wide Range of pH

Alka Rani[a], Rathindranath Biswas[b], Ayan Roy[c], Arnab Dutta[b], Harjinder Singh[a],*

[a]Department of Chemistry, Maulana Azad National Institute of Technology, Bhopal-462003, Madhya Pradesh, India.

[b]Chemistry Department Indian Institute of Technology Bombay, Mumbai 400076, Maharashtra, India.

[c]Department of Pure and Applied Physics, Guru Ghasidas Vishwavidyalaya (CU), Koni, Bilaspur 495009, India.

Email of corresponding author: harjinder@manit.ac.in

1. Mechanism of HER and OER

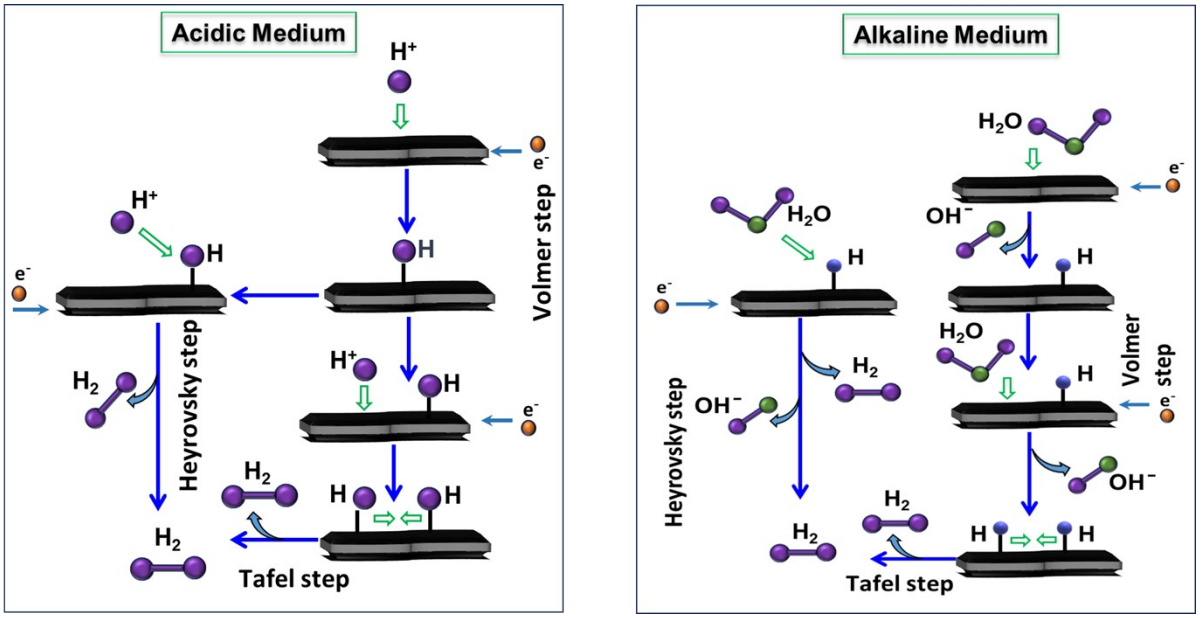

Scheme S1. Mechanism of Hydrogen Evolution Reaction (HER) in acidic and alkaline medium

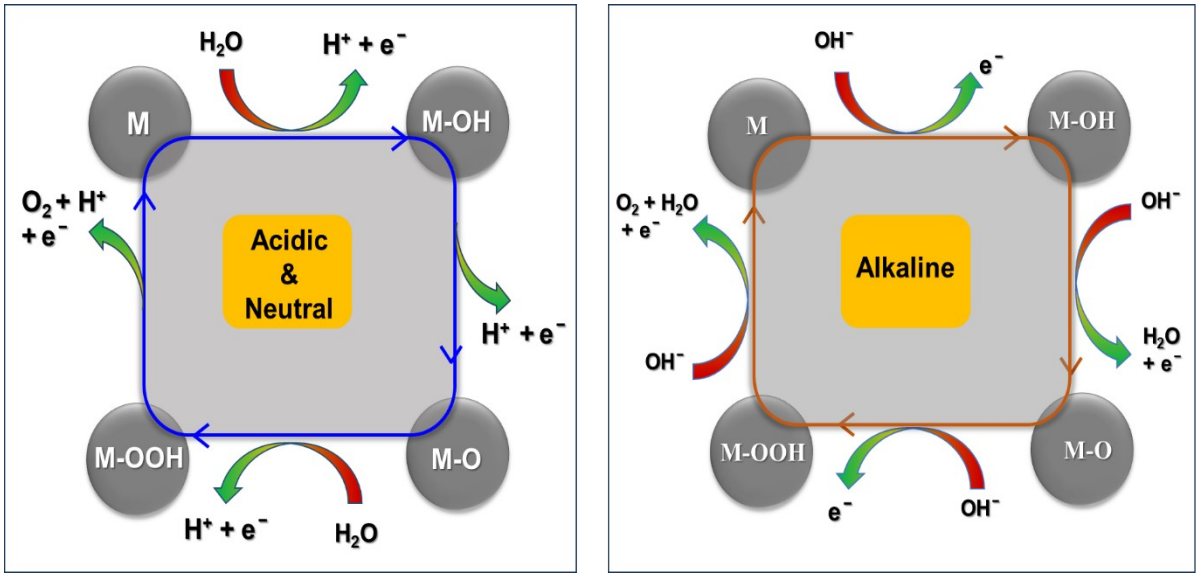

Scheme S2. Mechanism of Oxygen Evolution Reaction (OER) in acidic and alkaline medium

2. Characterisations:

The crystalline phase and structural integrity of the synthesized Ni/NiO heterostructures were recorded using a Rigaku X-ray diffractometer with Cu – kα source at a scan rate of 4° min^{-1} with Cu Kα radiation (λ = 0.15406 nm) and step size of 0.02°. To gain deeper insight into the structural and morphological features of the material, high-resolution transmission electron microscopy (HRTEM) analysis was carried out by transmission electron microscopy (TEM) from Thermo Scientific, Themis S2300 G3 microscope (300 kV). For TEM analysis, a dilute dispersion of the sample in toluene was drop-cast onto a carbon-coated copper grid, followed by solvent evaporation under ambient conditions. Chemical states and electronic environments of Ni and O species were analysed by X-ray photoelectron spectroscopy (XPS) on Axis Supra spectrometer (Kratos Analytical) with a Monochromatic Al Kα source. Electrochemical measurements relevant to the hydrogen evolution reaction (HER) and oxygen evolution reaction (OER) were performed using a Metrohm Autolab Multichannel-204 electrochemical workstation controlled via Nova 2.1.4 software.

Table S1. Structural parameters of Ni/NiO heterostructures obtained from Rietveld refinement pattern fitting.

Sample Composition	**Phases**	**Atoms**	**Oxidation state**	**Wyckoff notation**	**Positional coordinates x = y = z**	**U_{iso}**	**Occupancy**	**Bond length (Å) & Bond Angles**
Ni/NiO	NiO (70.51 %)	Ni1	2^+	4b	0.5000	0.084	1.00	Ni1–O1 = 2.09096 $\angle O1-Ni1$ = 90º
		O1	2^-	4a	0.000	0.084	1.00	
		Crystal system = face-centered cubic, lattice parameters: a = b = c = 4.18192 Å; cell volume = 73.135322 $Å^3$, space group = Fm-3m (#225). Bragg R Factors: R_{Bragg} = 2.25, R_F = 2.91						

	Ni (29.49 %)	Ni1	0	4a	0.0000	0.145	1.00	
		Crystal system = face-centered cubic, lattice parameters: a = b = c = 3.52631 Å; cell volume = 43.849178 Å^3, space group = Fm-3m (#225). Bragg R Factors: R_{Bragg} = 3.84, R_F = 11.2 Conventional Rietveld R-Factors: R_p = 30.2, R_{wp} = 18.3, R_{exp} = 18.16, χ^2 = 1.02						

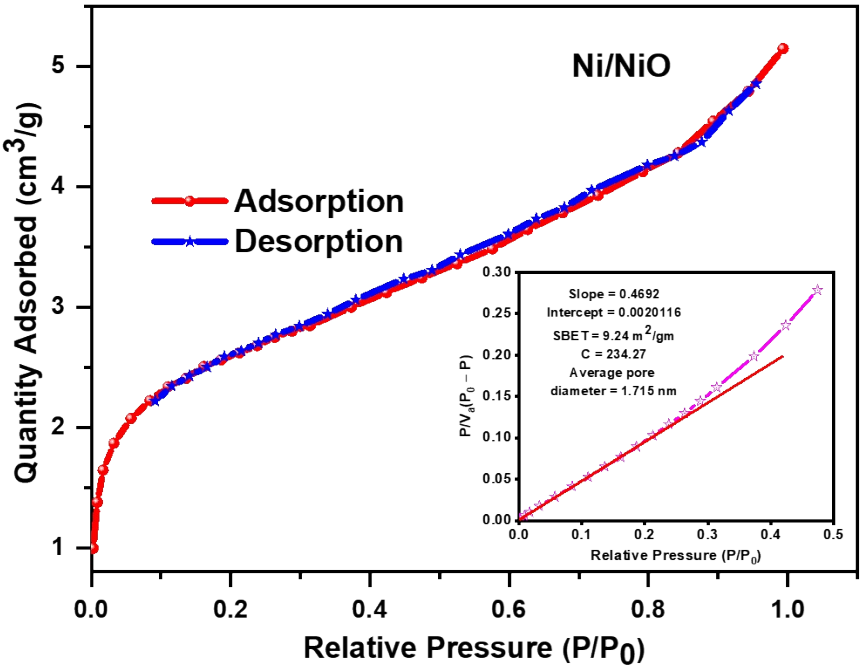

Figure S1. N_2-Adsorption-desorption isotherm of Ni/NiO.

3. Procedure for Electrochemical OER and HER Measurements:

The electrochemical experiments were successfully carried out in a Metrohm Autolab (Multichannel-204) electrochemical station, that is coupled with the three-electrode system via

Nova 2.1.4 software. The as-prepared 30 µL catalyst ink was drop-coated onto the carbon paper (Gas Diffusion Layer), which engaged as working electrode, Hg/HgO acted as reference whereas Pt wire and graphite rod worked as counter electrode for OER and HER measurements, respectively. The electrochemical activity was using 1 M KOH solution, prepared with double distilled water and degassed by 30 minutes Argon gas purging in the electrolyte for both OER and HER performance. Linear sweep voltammetry (LSV) with a scan rate of 10 mV s^{-1} and the potential window range of 0.1 to -1 V vs Hg/HgO in 1 M KOH electrolytic solution was used to record the polarisation curve for HER while the OER activity was measured in a potential window range of 0 V to 1.1 V *vs.* Hg/HgO with 10 mV s^{-1} scan rate in 1 M KOH electrolytic solution. Cyclic voltammetry (CV) studies had been conducted with scan rates ranging from 40 mV/s to 120 mV/s in 0.0 V to 0.20 V (*vs.* Hg/HgO) potential range in 1 M KOH solution. In 1 M KOH solution, electrochemical impedance spectroscopy (EIS) was conducted over the frequency range of 100 kHz to 0.1 Hz at a different applied overpotential for both OER and HER.

All the potentials were converted to RHE using the following Nernst equation for OER activities:[1-3]

$$E_{(RHE)} = E_{W\ vs.Hg/HgO} + 0.059pH + E_{Ref\ (Hg/HgO,\ 1\ M\ KOH)} \quad \text{--------- (S1)}$$

Where, E_W represents the potential of working electrode. E_{Ref} indicts the potential the of the corresponding reference electrode.

The electrochemically active surface area (ECSA) is directly proportional to the electrochemical double layer capacitance (C_{dl}) and it is calculated by applying below equation[4]:

$$ECSA = C_{dl}/C_s \quad \text{--------- (S2)}$$

where C_s represents the specific capacitance of flat fabricated working electrode with a value of 40 μF cm^{-2} per cm^2_{ECSA}. The double-layer capacitance (C_{dl}) is calculated from the slope, of Δj vs. scan rate plot. Where, Δj represents the difference of J_a (anodic current density) or J_c (cathodic current density).

Further, the Tafel slope was determined from LSV curve using Tafel equation given below:

$$\eta = a + b \log j \text{ ---------- (S3)}\ ^{5}$$

where a is the Tafel constant, b corresponds to the Tafel slope and j means the measured current density.

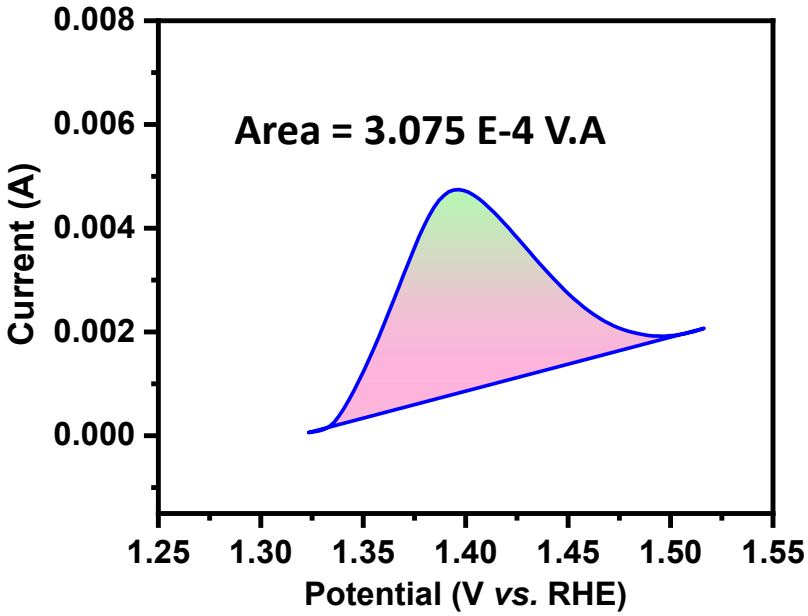

Figure S2. The area of the oxidation peak of Ni^{2+} to Ni^{3+} is considered for calculating the number of surface-active sites.

Table S2. The details of the electrochemical impedance spectra fittings are tabulated here.

EIS fitting details for OER:				
Applied overpotential (mV)	**R_s (Ohm)**	**R_{ct} (Ohm)**	**CPE (mMho.s^n)**	**χ^2**
340	5.4	12.7	3.4 and 35.8	0.03617
370	5.5	8.5	3.1 and 30.6	0.03092
400	5.3	6.6	3.3 and 28.7	0.03224
430	5.4	4.8	3.2 and 27.5	0.02540
460	5.2	3.6	2.7 and 26.7	0.02452
EIS fitting details for HER:				
Applied overpotential (mV)	**R_s (Ohm)**	**R_{ct} (Ohm)**	**CPE (mMho.s^n)**	**χ^2**
440	5.8	47.5	36.4 and 155.8	0.03754
470	5.7	29.3	33.4 and 100.5	0.03070
500	5.8	18.9	32.1 and 75.2	0.03261
530	5.7	8.5	31.5 and 36.6	0.02374

#Note: mMho represents millisiemens (mS)

4. Determination of Turn Over Frequency (TOF)

The TOF value for OER and HER experiments can be calculated as described in equation [6, 7](1)

$$TOF = \frac{j\,N_A}{F\,n\,\Gamma} \qquad \text{---------- (1)}$$

Where,

j = current density (mA cm^{-2}), N_A = Avogadro constant ($6.0221 \times 10^{23}\ mole^{-1}$), n is the number of electrons transferred = 4 for OER, 2 for HER, and Γ is the surface or total concentration of catalyst in terms of number of atoms.

The calculated area associated with the oxidation of Ni^{2+} to Ni^{3+} of both Compounds I and II, as depicted in Figure S2.

For **Ni/NiO**, the associated charge = $(3.075 \times 10^{-4}$ V.A)/ 0.01 V s^{-1}

$= 3.075 \times 10^{-2}$ A.s $= 3.075 \times 10^{-2}$ C.

Now, the number of electron transferred = $3.075 \times 10^{-2}\,C$ / $1.602 \times 10^{-19}\,C = 1.92 \times 10^{17}$

Since the oxidation of Ni^{2+} to Ni^{3+} is a single electron transfer reaction, the number of electrons calculated above is exactly the same as the number of surface-active sites for **Ni/NiO**.

TOF value of **Ni/NiO** at η = 350 mV for OER:

$$TOF_{1.66\,V} = \frac{j\,N_A}{F\,n\,\Gamma} = \frac{7.92 \times 10^{-3}\,A\,cm^{-2} \times (6.0221 \times 10^{23}\,atoms\,mole^{-1})}{96485\,s\,A\,mole^{-1} \times 4 \times (1.92 \times 10^{17}\,atoms\,cm^{-2})}$$

$TOF_{1.66\,V} = 6.4 \times 10^{-2}\ s^{-1}$

TOF value of **Ni/NiO** at η = 430 mV for HER:

$$TOF_{1.66\,V} = \frac{j\,N_A}{F\,n\,\Gamma} = \frac{9.22 \times 10^{-3}\,A\,cm^{-2} \times (6.0221 \times 10^{23}\,atoms\,mole^{-1})}{96485\,s\,A\,mole^{-1} \times 2 \times (1.92 \times 10^{17}\,atoms\,cm^{-2})}$$

$TOF_{1.66\,V} = 14.98 \times 10^{-2}\ s^{-1}$

Table S3. Turn over frequency (TOF) of Ni/NiO for OER and HER.

Overpotentials (mV) for OER	TOF ($\times 10^{-2}$ s^{-1}) for OER	Overpotentials (mV) for HER	TOF ($\times 10^{-2}$ s^{-1}) for HER
350	6.4	430	14.98
380	10.47	460	20.88
410	14.83	490	31.46
440	20.48	520	42.78
470	26.55	550	56.79
500	37.36	580	73.71

Table S4. Comparison table of TOF values of NiO-based reported catalyst with the present Ni/NiO catalyst for OER.

Catalysts	TOF calculated at the following overpotential	TOF (s^{-1})	Reference
Fe-doped NiO	~300 mV (0.1 M KOH)	0.05	[8]
$Ni(OH)_2$ nanoplates	490	0.21×10^{-2}	[9]
Ni/NiO nanoparticles	320 (1.0 M KOH)	0.11	[10]
NiO thinfilms	0.5 M KOH 360 mV	0.07	[11]
NiO hollow nanofibers	400 mV	3.9×10^{-2}	[12]
$Ni(OH)_2$ nanospheres	350 mV (0.1 M KOH)	0.036	[13]
NiTi oxide nanosheets	500 mV (1 M KOH)	0.068	[14]
Ni/NiO Composite	1 M KOH	0.064	**This work**

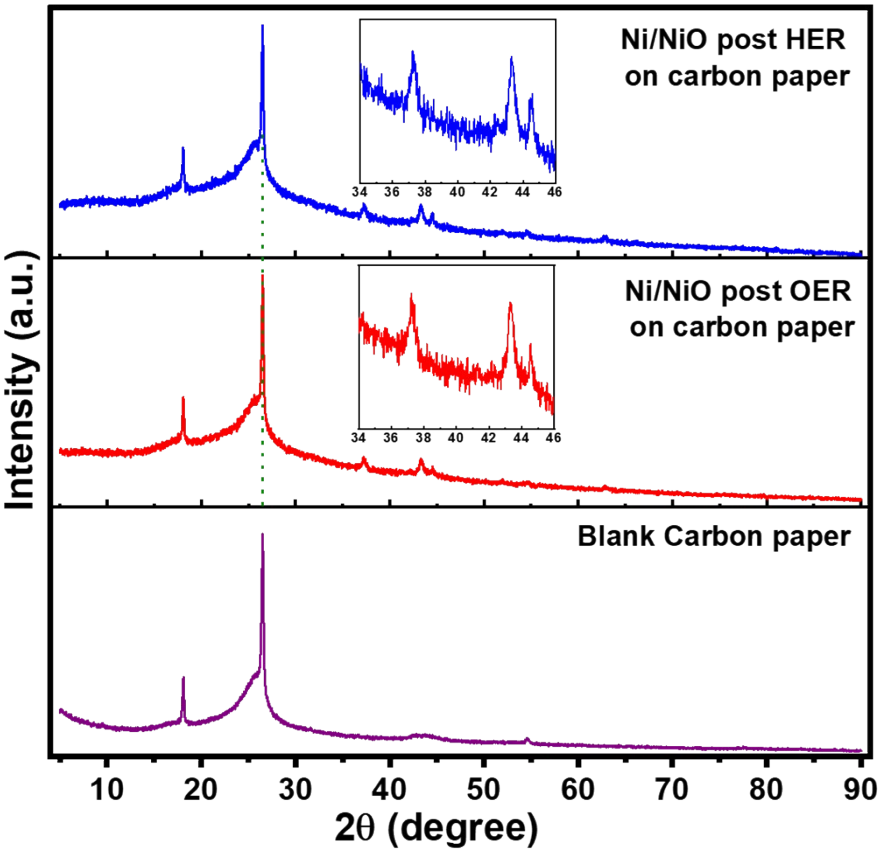

Figure S3. PXRD pattern of Ni/NiO Heterostructure on carbon paper after OER and post HER stability test.

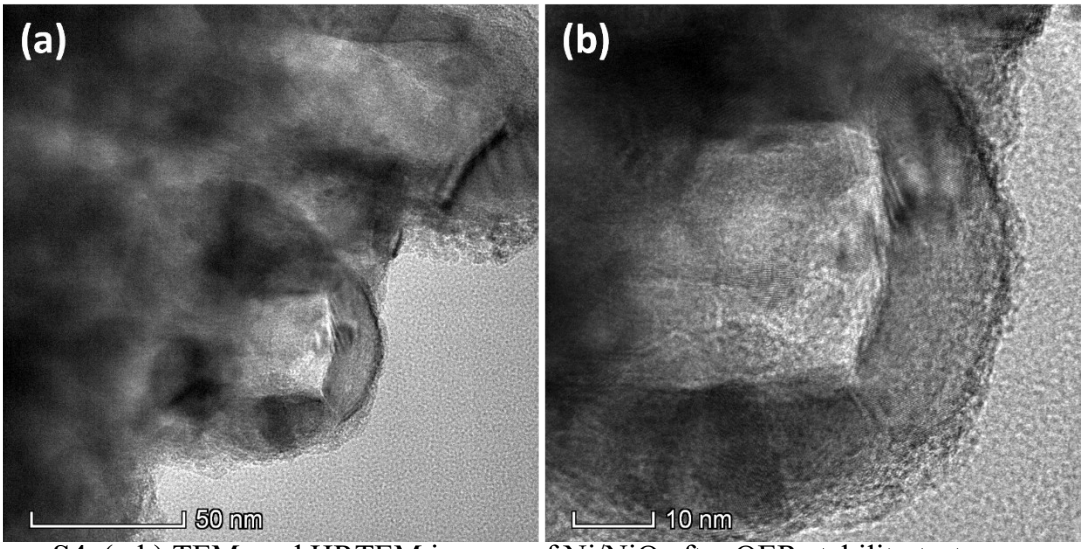

Figure S4. (a-b) TEM, and HRTEM images of Ni/NiO after OER stability test.

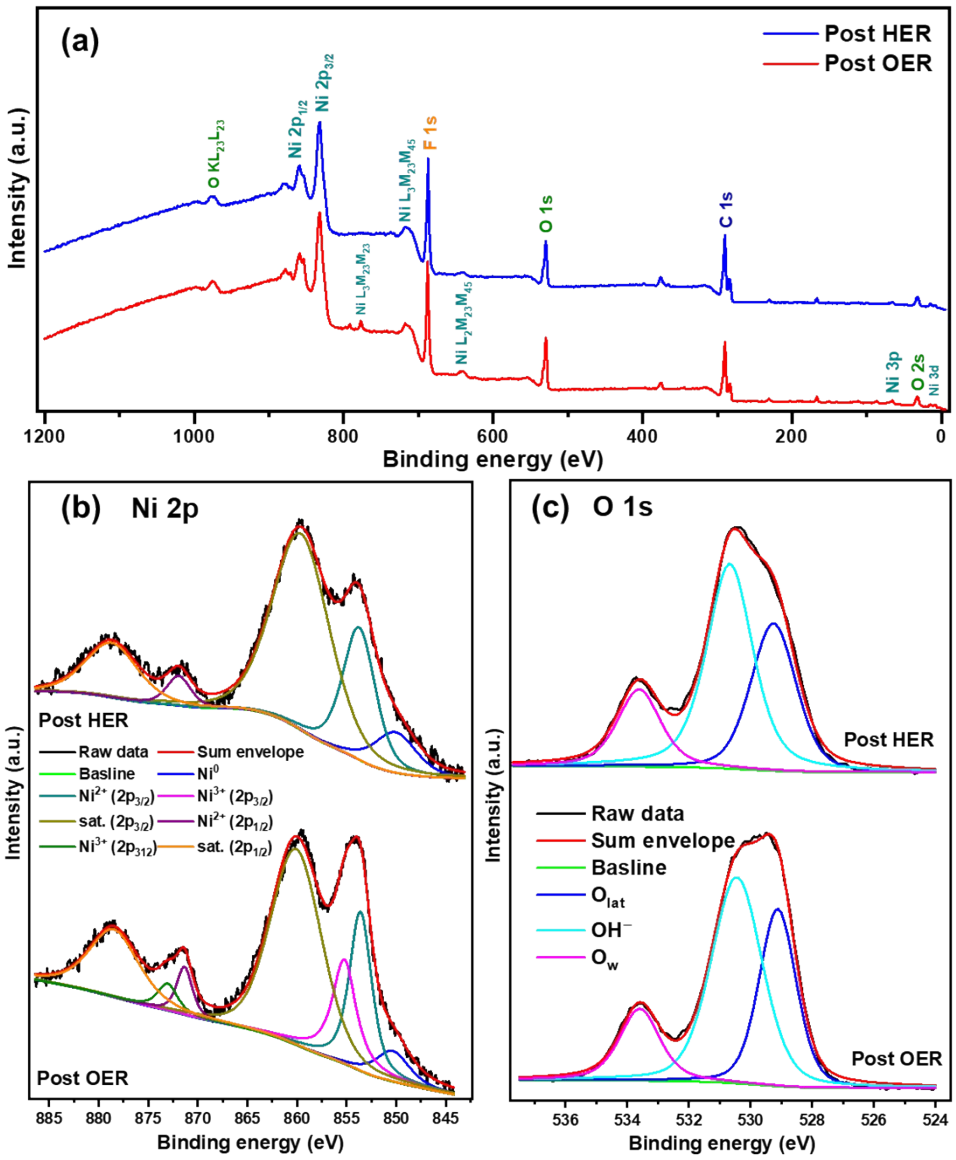

Figure S5. (a) XPS Survey spectra of post OER and post HER Ni/NiO heterostructures and the comparative peak fitted HRXPS spectra of (b) Ni 2p and (c) O 1s.

Table S5. Shows the comparative study of electrocatalytic performance of Ni/NiO nanostructures with metallic Ni and NiO_x based catalyst for OER and HER

Catalyst	Overpotential (mV) @10 mA/cm²		Tafel Slope (mV/dec)		Electrolyte		Ref.
	OER	HER	OER	HER	OER	HER	
NiO@Ni/WS_2/CC	347#	-	108.9	-	1 M KOH	-	[15]
Ni/NiO_x NPs	432	-	123	-	0.1 M KOH	-	[16]
NiO NA/CC (Nanosheet Array on Carbon Cloth)	422	-	116	-	1 M KOH	1 M KOH	[17]
Ni/NiO core–shell NWs on NF	382	146	103	72	1 M KOH	1 M KOH	[18]
NiO hollow microspheres (NiO-400)	470	498	188	145	1 M KOH	1 M KOH	[19]
NiOx/Ni	390	-	~69	-	1 M KOH	-	[20]
Carbon-Anchored NiO Nanotablets	320	-	49	-	1 M KOH	-	[21]
NiO nanoparticles/GO	625	453	168	128	1 M KOH	1 M KOH	[22]
2D porous NiO nanoplates	476	384	136	326	1 M KOH	0.5 M H_2SO_4	[23]
0D NiO nanoparticles	373	268	139	201	1 M KOH	0.5 M H_2SO_4	[23]
Ni/NiO	363	437	182	182	1 M KOH	1 M KOH	**This Work**

= at 50 **mA/cm²**

References:

1. T. Rom, R. Biswas, K.K. Haldar, S. Sarkar, U. Saha and A.K. Paul, *Inorg. Chem.* **2021,** *60* (20), 15106-15111.
2. M. Jiang, H. Zhai, L. Chen, L. Mei, P. Tan, K. Yang and J. Pan, *Adv. Funct. Mater.* **2023,** *33* (33), 2302621.
3. S.S. Sankar, A. Rathishkumar, K. Geetha and S. Kundu, *Energy Fuels* **2020,** *34* (10), 12891-12899.
4. C.C. McCrory, S. Jung, J.C. Peters and T.F. Jaramillo, *Chem. Soc.* **2013,** *135* (45), 16977-16987.
5. P. Mani, A. Sheelam, P.E. Karthik, R. Sankar, K. Ramanujam and S. Mandal, *ACS Appl. Energy Mater.* **2020,** *3* (7), 6408-6415.
6. N. Seal, A. Karmakar, S. Kundu and S. Neogi, *ACS Sustainable Chem. Eng.* **2022,** *11* (3), 979-993.
7. K. Karthick, S. Anantharaj, P.E. Karthik, B. Subramanian and S. Kundu, *Inorg. Chem.* **2017,** *56* (11), 6734-6745.
8. R.R. Rao, S. Corby, A. Bucci, M. García-Tecedor, C.A. Mesa, J. Rossmeisl, S. Giménez, J. Lloret-Fillol, I.E. Stephens and J.R. Durrant, *J. Am. Chem. Soc.* **2022,** *144* (17), 7622-7633.
9. X. Zhou, Z. Xia, Z. Zhang, Y. Ma and Y. Qu, *J. Mater. Chem. A* **2014,** *2* (30), 11799-11806.
10. F.E. Sarac Oztuna, T. Beyazay and U. Unal, *J. Phys. Chem. C* **2019,** *123* (46), 28131-28141.
11. A.C. Pebley, E. Decolvenaere, T.M. Pollock and M.J. Gordon, *Nanoscale* **2017,** *9* (39), 15070-15082.
12. V.D. Silva, T.A. Simões, J.P. Grilo, E.S. Medeiros and D.A. Macedo, *J. Mater. Sci.* **2020,** *55* (15), 6648-6659.
13. M. Gao, W. Sheng, Z. Zhuang, Q. Fang, S. Gu, J. Jiang and Y. Yan, *J. Am. Chem. Soc.* **2014,** *136* (19), 7077-7084.
14. Y. Zhao, X. Jia, G. Chen, L. Shang, G.I. Waterhouse, L.Z. Wu, C.H. Tung, D. O'Hare and T. Zhang, *J. Am. Chem. Soc.* **2016,** *138* (20), 6517-6524.
15. D. Wang, Q. Li, . Han, Z. Xing and X. Yang, *ACS Cent. Sci.* **2018,** *4* (1), 112-119.
16. B. Li, S.W. Chien, X. Ge, J. Chai, X.Y. Goh, K.T. Nai, T.A. Hor, Z. Liu and Y. Zong, *Mater. Chem. Front.* **2017,** *1* (4), 677-682.
17. N. Cheng, Q. Liu, J. Tian, X. Sun, Y. He, S. Zhai and A.M. Asiri, *Int. J. Hydrogen Energy* **2015,** *40* (32), 9866-9871.
18. H. Sun, Z. Ma, Y. Qiu, H. Liu and G.G. Gao, *Small* **2018,** *14* (31), 1800294.
19. A. Mondal, A. Paul, D.N. Srivastava and A.B. Panda, *Int. J. Hydrogen Energy* **2018,** *43* (47), 21665-21674.
20. G.Q. Han, Y.R. Liu, W.H. Hu, B. Dong, X. Li, X. Shang, Y.M.Chai, Y.Q. Liu and C.G. Liu, *Appl. Surf. Sci.* **2015,** *359*, 172-176.
21. S. Sekar, D.Y. Kim and S. Lee, *Nanomaterials* **2020,** *10* (7), 1382.
22. S.G. Jo, C.S. Kim, S.J. Kim and J.W. Lee, *Nanomaterials* **2021,** *11* (12), 3379.
23. V. Manjunath, S. Bimli, R. Biswas, P.N. Didwal, K.K. Haldar, M. Mahajan, N.G. Deshpande, P.A. Bhobe and R.S. Devan, *Int. J. Hydrogen Energy* **2022,** *47* (92), 39018-39029.